J. Fluid Mech. (1978), *vol.* 87, *part* 2, *pp.* 289–298
Printed in Great Britain

Stability of thin, radially moving liquid sheets

By DANIEL WEIHS

Department of Aeronautical Engineering, Technion – Israel Institute of Technology, Haifa

(Received 19 May 1977 and in revised form 6 February 1978)

An analysis of the stability of thin viscous liquid sheets, such as those emitted from industrial spraying nozzles, is presented. These sheets are in the form of a circular sector whose thickness reduces as the distance from the nozzle increases.

The Kelvin–Helmholtz type of instability usually observed causes the breakup and atomization of the sheet, as required in most industrial spraying processes. Waviness, like that of a flapping flag, is produced and increasing amplitudes finally cause breakup.

An analytical solution in the form of hypergeometric functions for the shape of the sheet and the waves is obtained. This solution includes, as special cases, analyses existing in the literature, in addition to establishing the possibility of a new type of instability dependent on the distance from the nozzle. Also, the classical type of instability, in which the waves increase with time, is examined and relations for unstable waves as a function of parameters such as the fluid viscosity, surface tension and sheet velocity are obtained. It is shown that there is no single wave that has a maximum growth rate, but that the wavenumber for maximum instability increases with the distance from the nozzle orifice.

1. Introduction

Spray nozzles appear in various applications in industrial practice such as fuel atomization, fire-fighting and spraying. Many of these nozzles emit a thin sheet of liquid or a two-phase mixture. This sheet is atomized and disintegrates into the required droplets either through a Kelvin–Helmholtz type of instability, when this exists, or through outside excitation.

Because of their wide applicability, the flow from fan-spray nozzles has received much attention and various hydromechanical models for the instability and breakup of the fluid sheet into droplets have been proposed. The basic study by Squire (1953) treats an inviscid liquid sheet of constant thickness with parallel streamlines. This was followed by similar studies (Hagerty & Shea 1955; Fraser *et al.* 1962) until Dombrowski & Johns (1963) produced an analysis including finite viscosity of the liquid and diminishing thickness of the sheet. However, a Cartesian co-ordinate system was used here too and later experiments (Crapper *et al.* 1973) have shown that the prediction of the above analysis, of exponentially increasing oscillations, is not usually obtained. More recently Clark & Dombrowski (1972) and Crapper, Dombrowski & Pyott (1975) have applied a second-order theory and a large amplitude theory, respectively, to try to achieve better predictions. These two studies were again based on parallel-sided flat sheets.

In real fan-spray nozzles, however, the sheet of fluid emitted usually has the shape

of a circular sector. Flow within the sheet is in the radial direction (Dombrowski, Hasson & Ward 1960). No tangential motions are usually noticeable except at the sheet edges, where surface tension causes a tangential contraction. This effect, which can even cause closure of the sheet (Taylor 1960) at low sheet velocities (large Weber numbers), does not affect the radial direction of the streamlines in the central part of the sheet.

Also, as a result of the radial spreading, conservation of mass requires a corresponding reduction in sheet thickness as it is observed (and can also be shown by energy arguments) that the velocity in the sheet stays constant. This reduction in thickness has been verified by Matsumoto & Takashima (1971).

The present study will attempt, therefore, to analyse the effects of the radial spreading and the resulting changes in thickness, as well as the surface tension and viscosity of the fluid sheet, on the stability. The last two characteristics have been found experimentally to have a significant influence on stability (Dombrowski *et al.* 1960) and so were included in the analysis.

Only antisymmetric (flapping) modes of instability are examined as previous analyses (Squire 1953; Fraser *et al.* 1962), as well as experiments (Crapper *et al.* 1973, 1975), show that this mechanism predominates in the present case, as opposed to the 'varicose' mode observed in axisymmetric jets.

2. Analysis

The initial unperturbed system is taken to be a circular axisymmetric thin liquid sheet expanding radially, such as that produced by two equal impinging cylindrical coplanar jets (Taylor 1960). The actual shape of the spray emitted from a typical nozzle is just a sector of this circular sheet, but owing to the radial streamlines observed (see §1) the influence of the edges on stability is neglected. Experiments (Clark & Dombrowski 1972) show that this simplifying assumption is well justified, at least for the high-speed atomizing sprays usually encountered in engineering practice.

A linearized analysis of antisymmetric perturbations of the sheet is performed. A cylindrical polar co-ordinate system (figure 1) is a natural choice. We now examine excursions of the sheet centre in the y direction as a result of the various forces acting on it in this direction. This approach is similar to that of Dombrowski & Johns (1963), who, however, used a Cartesian system in addition to making some unnecessary simplifications, which will be pointed out later.

Take a sheet which is moving with speed U through a stationary gas and whose thickness h varies as the reciprocal of distance from the origin (Matsumoto & Takashima 1971). The inertial force on an infinitesimal annular segment of length $r\,\delta\theta$ and width δr due to small lateral motions can be written as

$$F_{in} = -\frac{\partial}{\partial t}\left(\rho_l r\,\delta\theta\, h(r)\,\delta r \frac{\partial y}{\partial t}\right) = -\rho_l K \frac{\partial^2 y}{\partial t^2}\delta\theta\,\delta r, \tag{1}$$

where ρ_l is the liquid density, y is the distance normal to the sheet plane moved by the centre-line of the segment and $K = hr$ is a constant obtained from

$$\dot{Q} = \rho_l hrU\zeta = K\rho_l U\zeta, \tag{2}$$

where $\dot{Q}$ is the nozzle mass flow rate and ζ the included spray angle.

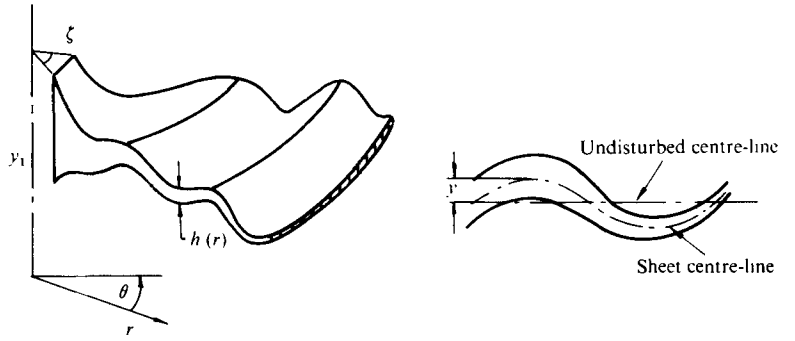

FIGURE 1. Schematic description of sheet and co-ordinate system.

Next we look at the force on an elementary volume due to surface tension. Only antisymmetric disturbances are examined here, far enough from the origin that the distance from the nozzle is large compared with the local sheet thickness.† The local slopes of the upper and lower surfaces are then approximately equal and the force due to surface tension is

$$F_{st} = \frac{\partial}{\partial r}(2\sigma r\,\delta\theta \sin\eta)\,\delta r, \tag{3}$$

where σ is the coefficient of surface tension and η is the local angle between the sheet and the undisturbed position of the centre-line. We are dealing with a small lateral disturbance, so that we can assume $\sin\eta \simeq \tan\eta$ and

$$F_{st} = \frac{\partial}{\partial r}\left(2\sigma r\,\delta\theta\frac{\partial y}{\partial r}\right)\delta r = 2\sigma\left(\frac{\partial y}{\partial r} + r\frac{\partial^2 y}{\partial r^2}\right)\delta\theta\,\delta r. \tag{4}$$

An additional factor producing forces in the y direction is the liquid's viscosity. As no variations in the tangential direction are allowed, the shear stress is

$$\sigma_{yr} = \mu\left[\frac{\partial}{\partial r}\left(\frac{\partial y}{\partial t}\right) + \frac{\partial}{\partial y}\left(\frac{\partial r}{\partial t}\right)\right] \tag{5}$$

for a fluid of viscosity μ. The second term in the square brackets is the result of the velocity profile in the sheet. This is a steady term which varies slowly with distance and will therefore be neglected here compared with the first term, which describes the resistance to wave production. Thus

$$F_v = \frac{\partial}{\partial r}\left(\frac{\partial^2 y}{\partial r\,\partial t} hr\,\delta\theta\right)\delta r = \frac{\partial}{\partial r}\left(\mu K\frac{\partial^2 y}{\partial r\,\partial t}\right)\delta r\,\delta\theta \tag{6}$$

and the net viscous force on the element is

$$F_v = \mu K\frac{\partial^3 y}{\partial r^2\,\partial t}\,\delta\theta\,\delta r. \tag{7}$$

Finally the effects of air pressure are determined. To obtain these effects we assume the viscous effects in the gas to be negligible and find the potential of the gas motions

† $h = K/r$ from (2), so that $dh/dr = -K/r^2 = -h/r$. The sheet thickness is typically of the order of 10^{-3} cm at 1 cm from the orifice, so that $dh/dr = O(10^{-3})$ there.

produced by the wavy sheet. Crapper *et al.* (1975) have suggested that the gas viscosity plays a part in the further, large amplitude development of the waves through large-scale vortex shedding and production of a vortex street in the air. This, however, is typical of a later stage in the instability and can be neglected during the initial stages which are studied here.

The perturbation potential can be written, following Squire (1953), in the form

$$\phi = Y(y_1)\,R(r)\exp[in(r-Ut)], \tag{8}$$

where n is a wavenumber and y_1 the distance from the undisturbed sheet centre-line. The unknown functions $Y(y_1)$ and $R(r)$ are obtained from Laplace's equation, which the velocity potential must satisfy. After separation of the variables and a sequence of standard substitutions (Kamke 1967, chap. C), one obtains for the upper surface, recalling that this perturbation decays for $y_1 \to \infty$,

$$Y(y_1) = Z_0 \exp(-ny_1) \tag{9}$$

and

$$R(r) = \exp(-inr)\,[C_1 J_0(nr) + C_2 Y_0(nr)], \tag{10}$$

where J_0 and Y_0 are Bessel functions of the first and second kind, respectively, and Z_0, C_1 and C_2 are constants. The potential is finite at $r = 0$ so $C_2 = 0$. Finally, substituting in (8) we obtain

$$\phi = \phi_1 \exp[-(ny_1 + inUt)]\,J_0(nr). \tag{11}$$

The pressure gradient can be related to the acceleration of the air (Dombrowski & Johns 1963), so that when speeds are low compared with the speed of sound in air, the pressure difference due to the wavy motion is obtained by integration:

$$P(y_1) = -\int_{\infty}^{y_1} \rho_g \frac{\partial}{\partial t}\frac{\partial \phi}{\partial y_1}\,dy_1 = -\rho_g \frac{\partial \phi}{\partial t}, \tag{12}$$

where ρ_g is the gas density. The pressure is now written in terms of the vertical (y_1) displacement, which is defined in terms of the velocity potential as

$$d = \frac{\partial}{\partial y_1}\int_0^t \phi\,dt_1, \tag{13}$$

where t_1 is a dummy time variable. Applying (13) to (11) and substituting in (12) gives

$$P = -\rho_g d U^2 n. \tag{14}$$

The net pressure on a point of the sheet is

$$P_l - P_u = \rho_g n U^2 [y + y] = 2\rho_g n U^2 y, \tag{15}$$

where l and u stand for the lower and upper surfaces respectively. The force on the element due to pressure differences caused by the waves is therefore

$$F_p = 2\rho_g n U^2 y r\,\delta r\,\delta\theta. \tag{16}$$

By summing (1), (3), (7) and (16) we obtain the force balance in the y direction. After simplification this is

$$2\rho_g n U^2 y r + \mu K \frac{\partial^3 y}{\partial r^2\,\partial t} + 2\sigma\left[\frac{\partial y}{\partial r} + r\frac{\partial^2 y}{\partial r^2}\right] - \rho_l K \frac{\partial^2 y}{\partial t^2} = 0. \tag{17}$$

Before going on to examine stability we first look for a general solution to this equation. This will help to give an idea of the form of waves produced by outside disturbances.

The solution is obtained by separation of the variables:

$$y = R(r)\,T(t). \tag{18}$$

Equation (17) now takes the form

$$2\rho_g n U^2 r + \mu K \frac{R''}{R}\frac{T'}{T} + 2\sigma\left[\frac{R'}{R} + r\frac{R''}{R}\right] - \rho_l K \frac{T'''}{T} = 0 \tag{19}$$

and we can write

$$\rho_l K T''/T = \lambda^2, \tag{20}$$

where λ^2 is a constant. As a result, if we take $\lambda^2 > 0$ so that unstable solutions may be obtained,

$$T = C_3 \exp\left(\frac{\lambda t}{(\rho_l K)^{\frac{1}{2}}}\right) + C_4 \exp\left(\frac{-\lambda t}{(\rho_l K)^{\frac{1}{2}}}\right). \tag{21}$$

We now choose the only solution which can result in an instability, i.e. put $C_4 = 0$. Then the equation for R reads, after some further manipulations,

$$(r+\Omega)R'' + R' + (\alpha r - \lambda_1^2)R = 0, \tag{22}$$

where

$$\Omega \equiv \frac{\mu\lambda}{2\sigma}\left(\frac{K}{\rho_l}\right)^{\frac{1}{2}}, \quad \alpha = \frac{\rho_g U^2 n}{\sigma}, \quad \lambda_1^2 = \frac{\lambda^2}{2\sigma}.$$

Equation (22) is a variant of the confluent hypergeometric equation and can be transformed into the standard form (Erdélyi *et al.* 1953, vol. 1, p. 249) by substituting

$$R = e^{sr}u(z), \quad z = -i2\alpha^{\frac{1}{2}}(r+\Omega), \quad s = i\alpha^{\frac{1}{2}}.$$

This gives

$$z\frac{d^2u}{dz^2} + (1-z)\frac{du}{dz} - \left(\tfrac{1}{2} + i\frac{\Omega\alpha + \lambda_1^2}{2\alpha^{\frac{1}{2}}}\right)u = 0 \tag{23}$$

and the solution of (22) is

$$R = C_5 \exp(i\alpha^{\frac{1}{2}}r)\, M\left[\tfrac{1}{2} + i\frac{\Omega\alpha + \lambda_1^2}{2\alpha^{\frac{1}{2}}},\ 1,\ -i2\alpha^{\frac{1}{2}}(r+\Omega)\right], \tag{24}$$

where M is Kummer's function of the first kind. Equations (21) and (24) constitute the full solution of (17), as the Kummer function of the second kind is obtained in logarithmic form when the second parameter is unity and is therefore unbounded for $r = 0$ and $\lambda = 0$. The other three M functions obtainable via Kummer's transformation are identical for our case of a second parameter of unity. The mathematical difficulty of further analysis of stability is highlighted by the fact that both the temporal amplification factor λ and the wavenumber n appear in the first parameter of the confluent hypergeometric function M. Varying either of these quantities causes a change in the nature of the resulting functions. Thus different periodic, or aperiodic, spatial dependences R can be obtained when λ or n is changed. This is reminiscent of the experimental findings reported by Crapper *et al.* (1973, 1975), where both the wave form and the amplification changed during the spatial development of the instability.

Some cases of interest can be obtained directly from (24). Looking first for possible bounds of stable regions, we take λ_1 to be zero, i.e. consider a temporal stability limit.

In this case we have $M(\frac{1}{2}, 1, -2i\alpha^{\frac{1}{2}}r)$, which is (Abramowitz & Stegun 1965, chap. 13) a product of an imaginary exponential and the Hankel function of order zero and the first kind: $H_0^{(1)}[\alpha^{\frac{1}{2}}r]$. The corresponding value N of the wavenumber is found from the argument of the Hankel function, which, as $\lambda = 0$, is

$$N = \rho_g U^2/\sigma. \tag{25}$$

This result coincides with the largest possible wavenumber for instability found by Dombrowski & Johns (1963) for a rectangular viscous spray. We see, therefore, that the bound of the time-stable wavelengths stays the same for the cylindrical geometry, while the related spatial dependence is now of Bessel-function shape, i.e. the cylindrical geometry will cause spatial decay of the temporal limit-cycle wave amplitude.

The far-field solution of (23) for large z (which corresponds to large r) is obtained by means of the asymptotic expansion for large $|z|$ and fixed parameters (Erdélyi *et al.* 1953, p. 278). The hypergeometric form (24) decays as $r^{-\frac{1}{2}}$ in the far field, i.e. purely spatial disturbances vanish far from the nozzles.

The general solution (24) includes, however, some intriguing further possibilities of unstable behaviour not apparent in the theoretical studies mentioned above. More general information on the behaviour of the function (24) can be obtained by means of the Sonine–Polya theorem (Szegö 1959, p. 164) without knowledge of its actual shape for different values of the parameters. Applying this theorem to (24), we find that successive maxima of R form an increasing sequence when $L(r) = (r+\Omega)(\alpha r - \lambda_1^2)$ is a decreasing, continuously differentiable function of r. This can be interpreted as a necessary condition for a different (spatial) type of instability. When the amplitudes of such successive maxima increase they may (but do not necessarily, i.e. this is not a sufficient condition) reach values where the sheet breaks down or nonlinear effects are obtained. Here this behaviour is called 'spatial instability', as it is independent of the temporal behaviour. Rewriting the expression for $L(r)$ above we have

$$L(r) = \alpha r^2 + (\Omega\alpha - \lambda_1^2)\, r - \Omega\lambda_1^2. \tag{26}$$

To find the range of r for which $L(r)$ is a decreasing function we observe that it is parabolic in r, i.e., for r smaller than the value r_c for which $dL/dr = 0$, L decreases. From (26)

$$r_c = \lambda^2/4\alpha\sigma - \tfrac{1}{2}\Omega \tag{27}$$

and when $r < r_c$ this kind of spatial instability is possible. On the other hand when

$$r > \lambda^2/4\alpha\sigma - \tfrac{1}{2}\Omega$$

the deformed spray sheet has decreasing maximum amplitudes as the distance from the origin increases, i.e. the asymptotic decay obtained above predominates. This is an interesting result which qualitatively agrees with the observations of Crapper *et al.* (1975), who found that waves on the sheet grew to a certain distance, being damped further away from the origin.

Writing out the expression for the critical radius r_c,

$$r_c = \frac{\lambda}{4}\left[\frac{\lambda}{\rho_g U^2 n} - \frac{\mu}{\sigma}\left(\frac{K}{\rho_l}\right)^{\frac{1}{2}}\right], \tag{28}$$

we see that the critical radius for spatial growth of disturbances depends strongly upon the temporal amplification factor. For positive λ (only real values of all quantities in

(28) are taken), i.e. temporally unstable cases, spatial instability in the present sense will occur when

$$\frac{\lambda}{\rho_g U^2 n} > \frac{\mu}{\sigma}\left(\frac{K}{\rho_l}\right)^{\frac{1}{2}}. \tag{29}$$

The case of negative real λ is of more interest. This ostensibly stable situation allows spatially increasing perturbations when

$$r_c < \frac{|\lambda|}{4}\left[\frac{|\lambda|}{\rho_g U^2 n} + \frac{\mu}{\sigma}\left(\frac{K}{\rho_l}\right)^{\frac{1}{2}}\right], \tag{30}$$

i.e., the larger the temporal stability, the larger the region of possible spatial instability. The actual value of r_c can be up to the order of centimetres for typical industrial low-pressure sprays, decreasing with increasing sheet velocity.

3. Approximate solution for the far field

The general considerations of the previous section have enabled us to establish bounds for stability in both the temporal and the spatial sense. However, owing to the complicated form of (24), it seems that generalizations of the other results of the simplified analyses mentioned in the introduction will be extremely tedious. Previous studies of stability placed great importance on the 'wavelength of maximum instability', i.e. when λ attains its greatest positive real value. This wavelength served as a basis for estimates of the size of ligaments torn off the sheet, which then dissipate into droplets. This model has however been disputed recently by Crapper *et al.* (1975). The present results tend to confirm their arguments, as there will not be a single periodic function with maximum amplification for the whole sheet, so that the dominant wave will depend on its point of origin in addition to being distorted.

Next, we examine an approximation to the case studied in the previous section, in order to show the relation between the present general solution and previous results.

The model is simplified by assuming the changes in thickness to be negligible. This is typical of the region far from the nozzle [see paragraph following (2)]. The force equation has to be rewritten, as (6) takes the form

$$F_v = \frac{\partial}{\partial r}\left[\mu H \frac{\partial^2 y}{\partial r\,\partial t} r\,\delta\theta\right]\delta r = \mu H\left[\frac{\partial^2 y}{\partial r\,\partial t} + r\frac{\partial^3 y}{\partial r^2\,\partial t}\right]\delta\theta\,\delta r, \tag{31}$$

where H is the now constant thickness of the layer. Equations (1), (3) and (16) remain unchanged, so that the equation for forces in the y direction is now

$$2\rho_g n U^2 y r + \mu H\left[\frac{\partial^2 y}{\partial r\,\partial t} + r\frac{\partial^3 y}{\partial r^2\,\partial t}\right] + 2\sigma\left(\frac{\partial y}{\partial r} + r\frac{\partial^2 y}{\partial r^2}\right) - \rho_l H r\frac{\partial^2 y}{\partial t^2} = 0. \tag{32}$$

Separating variables as in (18) one obtains

$$2\rho_g n U^2 + \left(\mu H\frac{T'}{T} + 2\sigma\right)\left(\frac{1}{r}\frac{R'}{R} + \frac{R''}{R}\right) - \rho_l H\frac{T''}{T} = 0. \tag{33}$$

The solution for T is identical to (21) with H replacing K and the equation for R is

$$R'' + \frac{1}{r}R' + \frac{2\rho_g n U^2 - \lambda^2}{\mu H\lambda/(\rho_l H)^{\frac{1}{2}} + 2\sigma} R = 0, \tag{34}$$

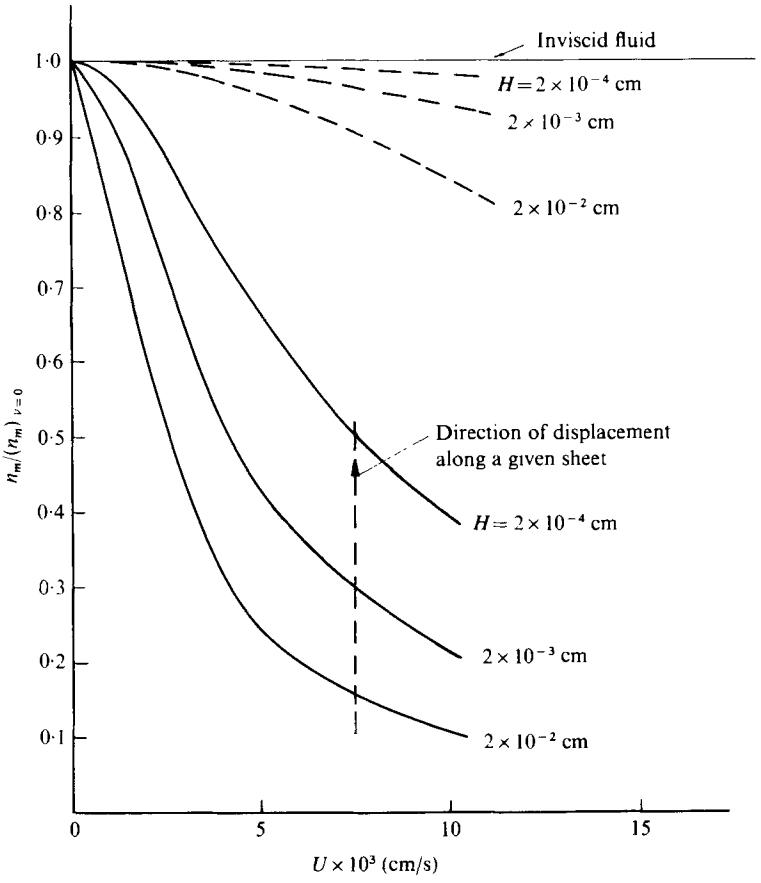

FIGURE 2. Ratio of wavenumber with maximum amplification factor to wavenumber with maximum amplification in an inviscid parallel-sided sheet *vs.* sheet velocity for various sheet thicknesses.

which is a Bessel equation, i.e. the far-field behaviour of (24) is retained. Thus

$$y = A_0 \exp\left[\lambda t/(\rho_l H)^{\frac{1}{2}}\right] J_0(rM^{\frac{1}{2}}),$$

where A_0 is a constant and M is the coefficient of R in (34). $M^{\frac{1}{2}}$ is then the wavenumber of the spatial dependence, so that a specific relation between λ and n can be found for this case:

$$\frac{2\rho_g n U^2 - \lambda^2}{\nu\lambda(\rho_l H)^{\frac{1}{2}} + 2\sigma} = n^2, \tag{35}$$

where ν is the kinematic viscosity of the sheet. Solving for λ gives

$$\lambda = \frac{\nu n^2 (\rho_l H)^{\frac{1}{2}}}{2}\left[-1 \pm \left(1 + \frac{8(\rho_g n U^2 - \sigma n^2)}{\nu^2 n^4 \rho_l H}\right)^{\frac{1}{2}}\right]. \tag{36}$$

Taking now the upper (positive square root) solution, inspection of (36) shows that $\lambda = 0$ (bound for stability) when $\rho_g n U^2 = \sigma n^2$, i.e.

$$n = \rho_g U^2/\sigma, \tag{37}$$

which is the same result as (25). In this case, however, further information may be obtained, since, when n increases above the value given by (37), λ becomes negative, so that (37) is an upper bound for unstable wavenumbers, i.e. wavelengths smaller than that obtained from (37) will be stable. The wavenumber n_m for which λ attains its largest real positive value is now plotted *vs.* velocity (figure 2), and can be seen to be a function of $H = \dot{Q}/(\rho_l r U \zeta)$, i.e. of distance also. As a result, for any finite viscosity, there will be a different 'wave of maximum instability' (obtained by moving vertically upwards on figure 2) with increasing wavenumber as the distance grows. The only case of a single wave of maximum instability is obtained when the sheet is inviscid. In that case n_m is, from (35),

$$n_m = \rho_g U^2/2\sigma, \tag{38}$$

which is identical with the result obtained by Squire (1953). Figure 2 is normalized by this value to enable comparison over a rather wide range of the parameters. The inviscid approximation is seen to be satisfactory for liquids of low viscosity such as water (dashed lines), for which even at very high velocities (100 m s^{-1}) the greatest change in the 'maximum' wavenumber is less than 20% when the distance changes by a factor of 100. On the other hand for viscous liquids (ν = 1 $cm^2 s^{-1}$, full lines) the wave of maximum instability as defined here is much longer than that predicted by (28) (smaller wavenumber) and the changes as one moves away from the nozzle are by a factor of two or more.

4. Conclusions

The analysis in §2 shows that the cylindrical expansion of the sheet emitted from fan-spray nozzles has a large influence on the stability, changing the form of the waves produced and their dimensions. The form of the waves, as well as the typical wavelength for instability and breakup, is dependent upon the original location of the disturbance, and deviations by a factor of 5 from predictions of the parallel-flow model are obtained (figure 2) for cases of practical interest. A new possibility of spatially growing waves is found, as a result of the characteristics of the hypergeometric function which describes the normal excursions of the sheet due to perturbations. It is not yet clear how and if this effect interacts with the time-dependent wave motion and an experimental programme to check this and other predictions of the present theory is now being carried out, as data in the literature do not usually contain all the required parameters.

REFERENCES

Abramowitz, M. & Stegun, I. A. 1965 *Handbook of Mathematical Functions*. Dover.

Clark, C. J. & Dombrowski, N. 1972 *Proc. Roy. Soc.* A **329**, 467–478.

Crapper, G. D., Dombrowski, N., Jepson, W. P. & Pyott, G. A. D. 1973 *J. Fluid Mech.* **57**, 671–672.

Crapper, G. D., Dombrowski, N. & Pyott, G. A. D. 1975 *Proc. Roy. Soc.* A **342**, 209–224.

Dombrowski, N., Hasson, D. & Ward, D. E. 1960 *Chem. Engng Sci.* **12**, 35–50.

Dombrowski, N. & Johns, W. R. 1963 *Chem. Engng Sci.* **18**, 203–214.

Erdélyi, A., Magnus, W., Oberhettinger, F. & Tricomi, F. G. 1953 *Higher Transcendental Functions*. McGraw-Hill.

Fraser, R. P., Eisenklam, P., Dombrowski, N. & Hasson, D. 1962 *A.I.Ch.E. J.* **8**, 672–680.

HAGERTY, W. W. & SHEA, J. F. 1955 *J. Appl. Mech.* **22**, 509–514.

KAMKE, E. 1967 *Differential-Gleichungen Lösungsmethoden und Lösungen*, 8th edn. Leipzig: Geest & Portig.

MATSUMOTO, S. & TAKASHIMA, Y. 1971 *J. Chem. Engng Japan* **4**, 257–263.

SQUIRE, H. B. 1953 *Brit. J. Appl. Phys.* **4**, 167–169.

SZEGÖ, G. 1959 *Orthogonal Polynomials*, 2nd edn. New York: Am. Math. Soc.

TAYLOR, G. I. 1960 *Proc. Roy. Soc.* A **259**, 1–17.